A Simulation Model for CO_2 Solar-Assisted Heat Pumps

Carlos Boabaid Neto[1], Samuel L. de Abreu[1], Joaquim M. Gonçalves[1], and Bruna de Noni[2]

[1] Federal Institute of Santa Catarina, São José Campus, São José (Brazil)

[2] Federal University of Santa Catarina, Araranguá Campus, Araranguá (Brazil)

Abstract

Heat pumps are a widely spread kind of thermal system used to provide heating. This kind of system has to be adapted to the new requirements related to environmental impacts of its working fluids. Several countries already restricted the use of non-environmental friendly fluids and established deadlines for the end of their use. Carbon dioxide is a suitable option since it is a natural substance, with very low greenhouse impact and null ozone depletion potential. Considering this scenario, a steady state simulation model was developed and a parametrical analysis is presented for a solar-assisted heat pump with carbon dioxide as working fluid on a transcritical compression cycle. In the high pressure side a gas cooler working as a counterflow heat exchanger provides hot water for residential use. In the low pressure side, a flat-plate solar collector improves heat input for the system enabling a more compact design. Simulation results are presented as a function of some working parameters that demonstrate the feasibility of the system for the intended application.

Keywords: solar assisted heat pumps, carbon dioxide, water heating.

1. Introduction

Electricity consumption for water heating in Brazil corresponds to approximately 20% of the demand of the residential sector. The electric shower is the main equipment used for this purpose (about 73% of the brazilian households). Due to population habits, the use of the electric shower increases the consumption at peak hours, which in turn demands costly measures by the electric sector (EPE, 2012). More economical and efficient alternatives are important in this context. Heat pumps are widely used for water heating worldwide (Buker and Riffat, 2016) and is an efficient solution (Sun et al., 2015), providing not only a much more efficient conversion of electric into thermal energy but also having the advantage of allowing thermal storage, shifting the peak of electric energy consumption. Due to Brazil's socioeconomical conditions, it is desirable that such systems be compact and of relatively low cost.

One of the strategies to improve the performance of heat pumps for water heating (HPWH) is to increase the heat supply on the cold side (heat sink). This can be achieved by the use of a solar-assisted heat pump (SA-HPWH) (Buker and Riffat, 2016), where a significant extra heat supply to the evaporator by solar irradiation enables a more compact and efficient system design.

The growing concern about the environmental impacts caused by human activity has led to a re-evaluation of materials and processes. In refrigeration the use of several fluids has been restricted since the discovery of the destructive effect of chlorofluorocarbons (CFCs) on the ozone layer in the 1970s, and the relationship between global warming and the increase of concentration levels of greenhouse gases in the atmosphere in the 1990s. International agreements and legislation now require replacing these refrigerants with others with low or null ozone depletion potential, less impact on the greenhouse effect and shorter atmospheric lifetimes (European Comission, 2007; Calm, 2008).

Carbon dioxide (CO_2) is one of the proposed working fluids for the new generation of heat pumps. It is a natural fluid with null ozone depletion potential and low greenhouse effect compared to other substances, non-flammable and non-toxic, presents good thermal properties, compatibility with common (mineral)

doi:10.18086/swc.2019.04.03 Available at http://proceedings.ises.org

lubricants, has low cost and do not need to be recycled (Lorentzen, 1995). All these advantages make it a good choice among the several existing refrigerant options, providing a totally safe, economical and cost-effective natural solution for heat pumps.

Indeed, CO_2 has been applied to heat pumps (Chen et al., 2016, Passos et al., 2017). Because of its low critical point, CO_2 application in HPWH cycles causes the fluid to operate under transcritical conditions, but the heat exchange with water can compensate for the reduction of efficiency resulting from the transcritical states when compared to a condensing refrigerant. CO_2 residential HPWH have been commercialized in Japan since 2001 (Zhang et al., 2015).

The present work aimed to evaluate through simulation the operation of a small SA-HPWH using CO_2 as the working fluid. Aiming at simplicity, an evaporator directly coupled to a flat-plate solar collector is proposed. This evaporator design is not common in CO_2 systems, making it an original feature.

2. Literature review

Studies involving the use of the heat pump for water heating have increased in the last decades. Hawlader et al. (2001) presented an analytical and experimental study on a SA-HPWH where an unglazed, flat plate solar collector acted as an evaporator for the refrigerant R-134a. Condenser was placed inside the hot water storage tank, heating a fixed mass of water. It was found that to ensure improved performance when the solar irradiance varies, a variable-speed compressor should be employed to allow a proper matching with the highly varying evaporator load and the thermostatic valve (TEV). Thermal performance of the system was affected significantly by speed of the compressor, solar irradiation, collector area and storage volume.

Sun et al. (2015) presented an experimental and numerical study on the comparison between a solar-assisted and a conventional air-source HPWH systems. The AS-HPWH employed a finned tube evaporator and TEV, while the SA-HPWH employed an unglazed, uninsulated roll-bond type evaporator, an electronic expansion valve and a smaller compressor. The use of a unglazed solar collector allowed to absorb heat from both solar radiation and ambient air, enabling the solar-assisted system to operate in all weather conditions all day. Both systems had the condenser placed inside the hot water tank. Results showed that the SA-HPWH showed better performance under clear day conditions (i.e., high radiative load), mostly because evaporating temperature of the system was increased. Also, SA-HPWH was capable of working adequately for low radiative load and even at overcast night condition, due to the convective heat transfer. The performance was significantly impaired only for clear night condition, due to the radiative heat loss.

Nawaz et al. (2018) presented a model to predict the performance of a HPWH that uses CO_2 as the refrigerant that was based on experimental data. The model was used to run a parametric analysis, and for a comparison with a R-134a HPWH. It was found that CO_2 HPWH performance was comparable to that of an R-134a HPWH when a gas cooler configuration was employed. This configuration resulted in much higher system performance for both refrigerants, even if it required additional infrastructure (water pump and flow control). The gas cooler was relatively larger for CO_2 than for R-134a, due to the single-phase vs. two-phase heat transfer, respectively. In such a configuration, the system was highly sensitive to the water circulation rate, and it was found that a system with a variable-speed pump had superior performance compared with a fixed-speed pump. The set point for water supply temperature also had a significant impact on the system performance, with a higher supply water set point degrading efficiency.

Paulino et al. (2019) presented a dynamic and distributed model of an evaporator of a direct expansion solar-assisted HPWH, in order to analyze the evaporator response to sudden changes in radiation. Experimental tests were performed and the comparison between experimental results and the model showed small deviations. The system was comprised of a gas cooler, a constant-speed compressor, a needle valve and a flat-plate collector evaporator. Simulations have shown that a step change in solar radiation produced relevant effects in the superheating at the evaporator outlet, indicating that an almost immediate action of the expansion device is necessary to correct it. Considering the small values for the time constants observed for the superheating step response and the fact that the system could operate in a continuous transient condition during some seasons, it was concluded that an electronic expansion valve (EEV) would be better suited to meet the needs of rapid interventions on the mass flow rate at the evaporator inlet.

The authors (De Noni et al., 2018) presented a parametric analysis of a HPWH operating on a transcritical CO_2 cycle, through simulation. The results showed that several features of the system must be improved to take advantage of the thermo-physical properties of the fluid and provide a better performance. It was shown that keeping the evaporator temperature close to the ambient temperature by adjusting the compressor speed yielded a higher COP, as well as increasing the superheating degree. The solar irradiance and the temperature of the water to be heated had great impact on the system performance, indicating that advanced control features must be employed to enhance the performance of the system under to varying demand.

3. System modeling

The lay-out of the proposed system is shown in Fig. 1(a), and operating conditions of refrigerant are shown in Fig. 1(b). Following the previous informations reported in Section 2, the system consists of a CO_2 heat pump with a flat plate solar collector evaporator and a counter flow heat exchanger – the gas cooler (GC) - to heat the water. A secondary hydronic system equipped with a variable-speed hydraulic pump is used to pump the water to and from an insulated tank. The use of an unglazed uninsulated flat plate solar collector as evaporator is proposed which yields low cost and allows the solar radiative thermal load to be summed to convective heat transfer with ambient air. The system is capable of operating at evaporating temperatures above or below the ambient air by the action of the variable-speed compressor, and a thermostatic expansion valve (TEV) is proposed as the expansion device. According to Fig. 1(b), at point 1 CO_2 leaves the evaporator in a superheated state. After an isentropic compression the fluid reaches transcritical condition (point 2) and enters the gas cooler, heating the water. The refrigerant leaving the gas cooler (point 3) undergoes an isenthalpic expansion process passing through the TEV, returning to the evaporator (point 4).

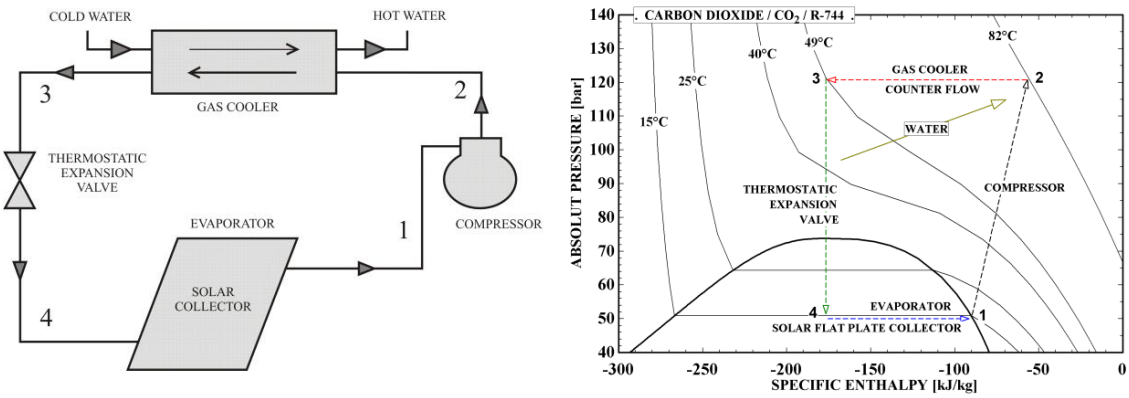

(a) **(b)**

Fig. 1: (a) heat pump configuration; (b) refrigeration cycle at pressure-enthalpy diagram.

System modeling was based on a similar model working with R134a (Abreu et al., 2011) that was later adapted to work with CO_2 (De Noni et al., 2018). The model solves a set of algebraic equations that describes the behavior of each component, based on mass and energy conservation principles under steady-state regime. Pressure drop and heat losses along piping and heat exchangers were considered negligible. All the variables are defined in Tables 1 and 2.

The compressor is modeled based on an isentropic compression process (eq. 1, 2) corrected by the use of compressor volumetric and isentropic efficiencies taken from experimental results of real compressors:

$$\dot{W}_{COMP} = \dot{m}_{CO2} * (h_{2S} - h_1)/\eta_g \qquad \text{(eq. 1)}$$

$$\dot{m}_{CO2} = ROT * V_{DISP} * \eta_v/v_1 \qquad \text{(eq. 2)}$$

where h_1 and h_{2s} are the enthalpies at point 1 and point 2, respectively. Compressor speed is not fixed, being instead a consequence of the refrigerant mass flow demanded. The expansion process is modeled as isenthalpic, and the expansion valve behavior is defined by setting the superheating degree at the evaporator outlet.

The solar collector is modeled considering factors for the optical efficiency and for thermal heat transfer to surrounding air (eq. 3, 4), both factors being obtained from manufacturers' data. The collector efficiency profile is considered to be valid for an evaporating temperature range above and below ambient temperature.

$$\dot{Q}_{EVAP} = G * A_{col} * \eta_{col} \quad \text{(eq. 3)}$$

$$\eta_{col} = F_R(\tau\alpha) - F_R U_L * (T_{EVAP} - T_{AMB})/G \quad \text{(eq. 4)}$$

The gas cooler (GC) was discretized in order to achieve a more realistic approach for CO_2 thermodynamic properties in the transcritical region, particularly near the critical point. The discretization scheme is shown in Fig. 2.

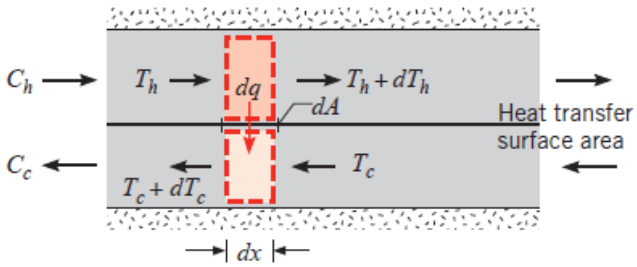

Fig. 2: Heat exchanger discretization (source: Incropera and De Witt, 1990)

The gas cooler is characterized by its global thermal conductance (UA_{GC}), that was assigned as input data, as well as the water inlet temperature ($T_{WATER,in}$). Both the water temperature rise ($\Delta T_{WATER} = T_{WATER,out} - T_{WATER,in}$) along the gas cooler or the water mass flow rate ($\dot{m}_{WATER}$) can be previously set. The solution is obtained through a finite difference scheme where the total enthalpy change of the refrigerant is equally divided and the corresponding value of UA_{GC} is calculated from conservation laws (eq. 5). The algorithm then iterates to find the solution for ΔT_{WATER} or $\dot{m}_{WATER}$, whichever is not previously set.

$$d\dot{Q}_{GC} = \dot{m}_{WATER} * c_{p,WATER} * dT_{WATER} = \dot{m}_{CO2} * dh_{CO2} = d(UA_{GC}) * (T_{CO2} - T_{WATER}) \quad \text{(eq. 5)}$$

The water mass flow rate is adjusted by the variable-speed hydraulic pump of the hydronic system, as suggested by Nawaz at al. (2018). Pump power was calculated in the usual way (Kakaç and Liu, 2002), taking into account viscous dissipation and considering typical technical data for this kind of system. However, quantitative results must be understood as purely indicative and not actual values. For this reason pumping power values were not included in the system COP calculation.

The expansion device was modeled as an isenthalpic process from point 3 condition (Fig.1(b)). In order to visualize the action of the expansion valve, the throat-area of the valve port (formed by the valve needle and seat) was calculated from (Li et al., 2004):

$$\dot{m}_{CO2} = C_V * A_{throat} * \sqrt{(p_{GC} - p_{EVAP})/v_3} \quad \text{(eq. 6)}$$

where A_{throat} is the throat-area, C_V is the discharge coefficient, and v_3 is the specific volume of CO_2 at the valve inlet.

Liao et al. (2000) presented a study on the optimization of the high pressure of a transcritical CO_2 cycle. The authors showed that, because of the peculiar thermodynamic and thermophysical properties of the CO_2 at transcritical conditions, there is an optimum pressure that will yield the maximum COP of the system, given by:

$$p_{high,optimum} = -9.34 + 0.381\ T_{EVAP} + 2.778\ T_3 - 0.0157\ T_{EVAP}\ T_3 \quad \text{(eq. 7)}$$

This optimum pressure is used to define the high pressure of the heat pump system. This is equivalent to defining, for each simulated condition, a certain appropriate refrigerant charge. In a real system this would require the use of a special expansion device (Peñarrocha et al., 2014, Montagner and Melo, 2014) consisting of two expansion valves and an accumulation tank, that would be capable of dynamically adjusting the amount of fluid circulating through the system. A simpler and cheaper alternative would be to adjust a single charge value to a high pressure slightly (5 to 10 bar) above the optimum pressure, which would allow proper system operation without significant performance degradation over a wide operating range. As a means of visualizing the optimum refrigerant charge, a simple model for charge estimation has been implemented, based on typical values for the inner volume of the high and low pressure sides of the system and the mean specific volume of the fluid in each side.

The computational model was developed with the Engineering Equation Solver (EES) software (Klein, 2002), employing the software own library of thermodynamic properties.

4. Results and discussion

A reference case was defined whose values are shown in Table 1. These values were chosen in a preliminary design of the system components based on a solar irradiance of 1,000 W m^{-2} and a solar collector area of 2 m^2. The volumetric displacement of the compressor (3.3 cm^3) and the global thermal conductance of the gas cooler (150 W K^{-1}) were estimated and then kept fixed for all calculations. Values for other parameters were typical operating conditions of a heat pump for water heating. Global and volumetric efficiency values for the compressor, as well as the values for optical efficiency and thermal losses factors of the solar collector are typical values for the operating range.

Solution of the model for the reference case yields the results presented in Tab. 2. As mentioned, compressor speed was adjusted according to the evaporating temperature set in order to satisfy the heat transfer rate in the solar collector, i.e., it is the variation of compressor speed that allows the proper evaporation pressure to be maintained even if there is a large variation in solar irradiance throughout the day. It can be seen that the results are realistic for such an application.

The behavior of the heat pump was analyzed for different control variables and operational conditions. Table 3 shows the parameters chosen and their working ranges. The temperature difference at the evaporator ($\Delta T_{EVAP} = T_{AMB} - T_{EVAP}$) and the superheating degree at the evaporator outlet were chosen as control variables since they are respectively related to the compressor speed and the expansion valve throttling. Solar irradiance and water temperature in the gas cooler inlet were the operational conditions. In all cases the gas cooler pressure was calculated to achieve the optimum system COP (eq. 7).

Figures 3 to 6 shows the results for the parametric analysis, where figures (a) shows the inlet and outlet temperatures and pressure of CO_2 at the gas cooler, (b) the mass flow rates of CO_2 and water in the gas cooler and the (computed) compressor speed, (c) the heat transfer rates, compressor work and COP of the heat pump, (d) the computed CO_2 charge and the expansion valve throat-area, and (e) the logarithmic mean temperature difference (LMTD, Incropera and De Witt, 1990) at the gas cooler and the pump power.

Tab. 1: Model input parameters for the reference case.

Component	Parameter	Symbol [unit]	Value
compressor	volumetric displacement	V_{DISP} [cm³]	3.3
	isentropic efficiency	η_g[-]	0.65
	volumetric efficiency	η_v[-]	0.75
gas cooler	overall thermal conductance	UA_{GC} [W K^{-1}]	150
	water temperature rise	ΔT_{WATER} [ºC]	10
	inlet water temperature	$T_{WATER,in}$ [°C]	40
solar collector	area	A_{COL} [m²]	2
	optical efficiency factor	$F_R(\tau\alpha)$ [-]	0.8
	thermal losses factor	F_RU_L [W m^{-2} K^{-1}]	10
	solar global irradiance	G [W m^{-2}]	1,000
	fluid/ambient temperature difference	ΔT_{EVAP} [ºC]	10
	superheating degree	SUP [ºC]	1
	ambient temperature	T_{AMB} [ºC]	25
fluid	carbon dioxide		

Tab. 2: Results for the reference case.

Parameter	Symbol [unit]	Value
Compressor speed	ROT [rpm]	3,129
Pressure at gas cooler (refrigerant side)	p_{GC} [bar]	121.2
Evaporating pressure	p_{EVAP} [bar]	50.9
CO_2 temperature at compressor discharge	T_{2S} [°C]	82.2
CO_2 temperature at gas cooler outlet	T_3 [°C]	49.1
CO_2 mass flow rate	$\dot{m}_{CO2}$ [kg h^{-1}]	72.9
Water mass flow rate	$\dot{m}_{WATER}$ [kg h^{-1}]	209.8
Heat transfer at evaporator/collector	$\dot{Q}_{EVAP}$ [W]	1,800
Heat transfer rate at gas cooler	$\dot{Q}_{GC}$ [W]	2,439
Compressor power	$\dot{W}_{COMP}$ [W]	983
Heat pump coefficient of performance	COP [-]	2.48

Fig. 3 presents the results for the variation of ΔT_{EVAP}. One can see from Fig. 3(c) that the maximum COP is obtained for null difference, that is, when the evaporating temperature is equal to ambient temperature. Indeed, when T_{EVAP} is higher than T_{AMB} there is heat loss from the evaporator to the air, and for the reference

ambient temperature set (25 °C) these conditions resulted in the CO_2 being next to critical condition, which would degrade the heat transfer capacity in the evaporator, a situation not foreseen in the modeling, so it is to be expected that the reduction in COP would be even greater.

Tab. 3: Parameters and working ranges used for the parametric analysis.

Parameter	Symbol [unit]	Range
Evaporator temperature difference	ΔT_{EVAP} [ºC]	-5 a +10
Superheating degree	SUP [°C]	1 to 10
Solar irradiance	G [W m^{-2}]	200 to 1,100
Water inlet temperature at the gas cooler	$T_{WATER,in}$ [°C]	30 to 50

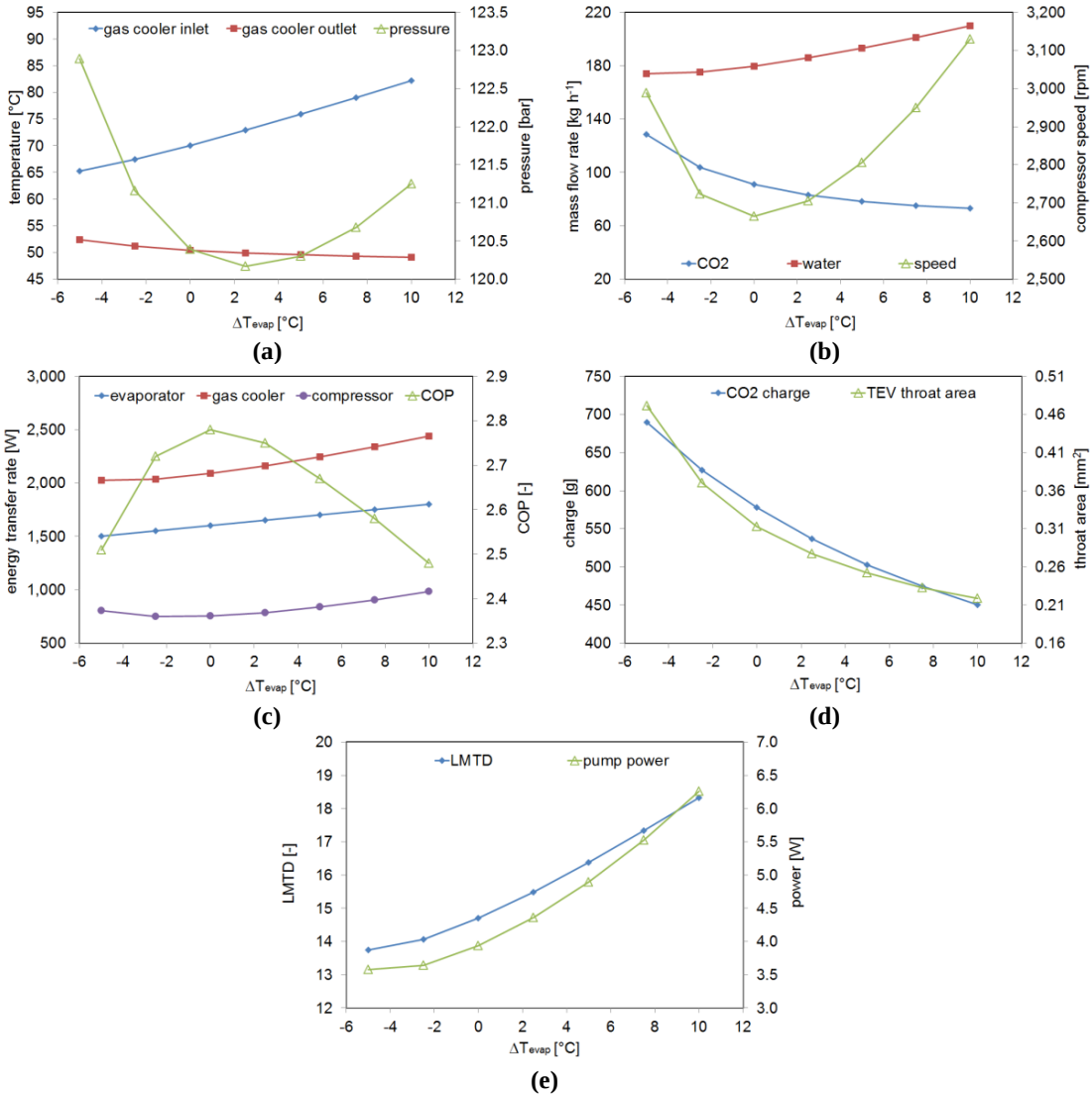

Fig. 3: Results for variation of ΔT_{EVAP} : (a) temperatures and pressure at gas cooler; (b) mass flow rates and compressor speed; (c) heat transfer rates, compressor power and COP; (d) expansion valve aperture and refrigerant charge; (e) LMTD and pump power.

When T_{EVAP} is lower than T_{AMB} the additional heat gain at the evaporator does not compensate for the increase of compressor power due to the increased pressure ratio. As ΔT_{EVAP} increases (i.e., T_{EVAP} decreases) there is an increase of the heat transfer at the gas cooler, and consequently an increase of the water mass flow rate and the pump power. Interestingly, in order to keep both T_{EVAP} and SUP constant, CO_2 mass flow rate must be reduced (and the expansion valve throat-area is reduced accordingly) but nevertheless compressor speed is increased (Fig. 3(b)) to overcome not only the increased pressure ratio but also the reduction of the specific volume at the compressor inlet. Variation of the predicted optimum pressure is relatively small (Fig. 3(a)) but CO_2 charge is strongly affected. The increase in the compressor discharge temperature (gas cooler inlet temperature) yields an increasing LMTD.

Fig. 4 presents the results for the variation of the superheating degree at evaporator outlet. As SUP increases the compressor speed reduces as a means of maintaining T_{EVAP} constant, and consequently there is a reduction in CO_2 mass flow rate and a small decrease of the heat transfer at the gas cooler, that is compensated by a stronger decrease of compressor power, resulting in a significant increase in the system COP. The refrigerant charge is also greatly reduced.

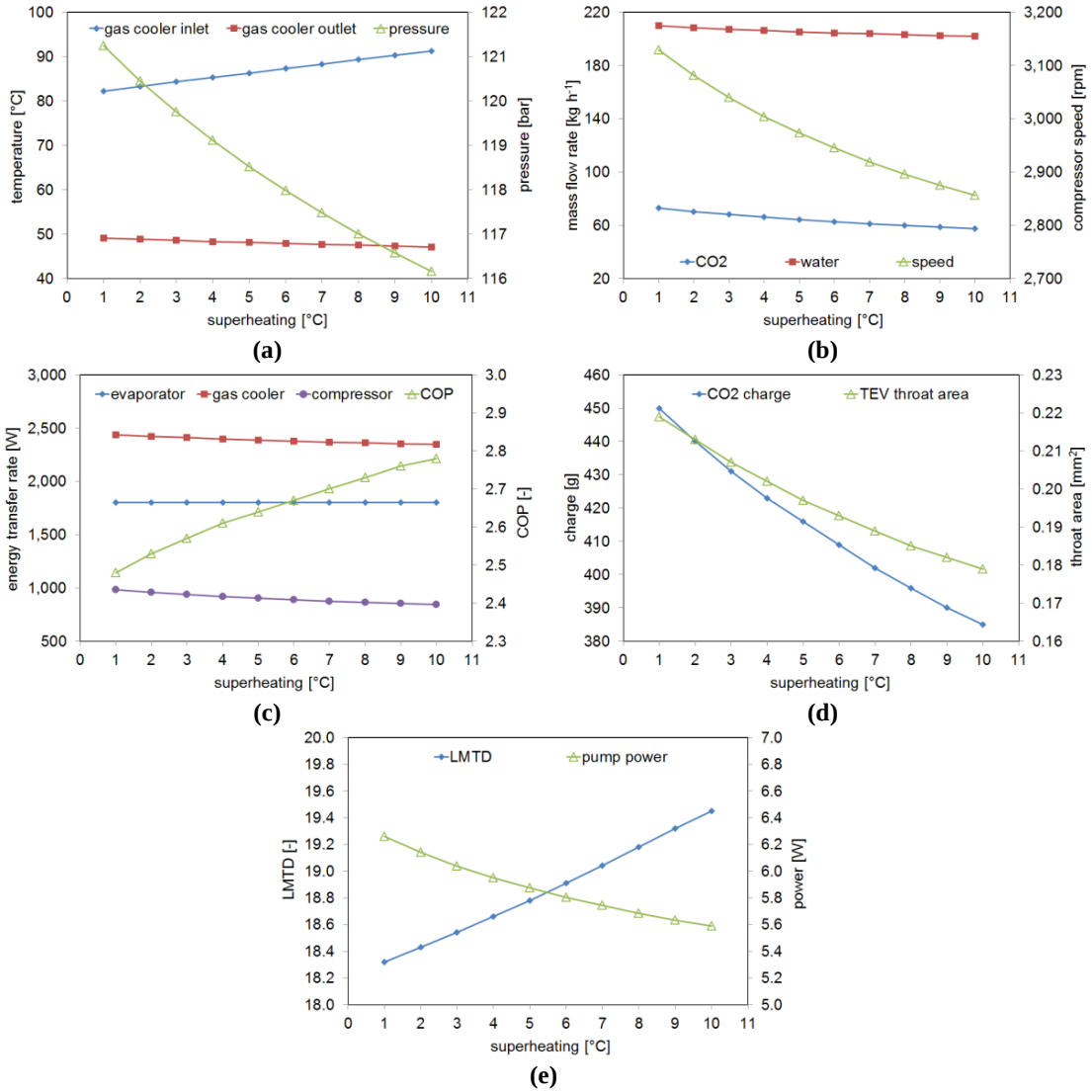

Fig. 4: Results for variation of the superheating degree: (a) temperatures and pressure at gas cooler; (b) mass flow rates and compressor speed; (c) heat transfer rates, compressor and pump power and COP; (d) expansion valve aperture and refrigerant charge; (e) LMTD and pump power.

Fig. 5 shows the results for the variation of the solar irradiance. As G increases the compressor speed also increases as a means of maintaining T_{EVAP} constant, also increasing the CO_2 mass flow rate and therefore the heat transfer at the gas cooler, but due to the even greater increase in compressor power, the COP is reduced. Other variables behaved accordingly.

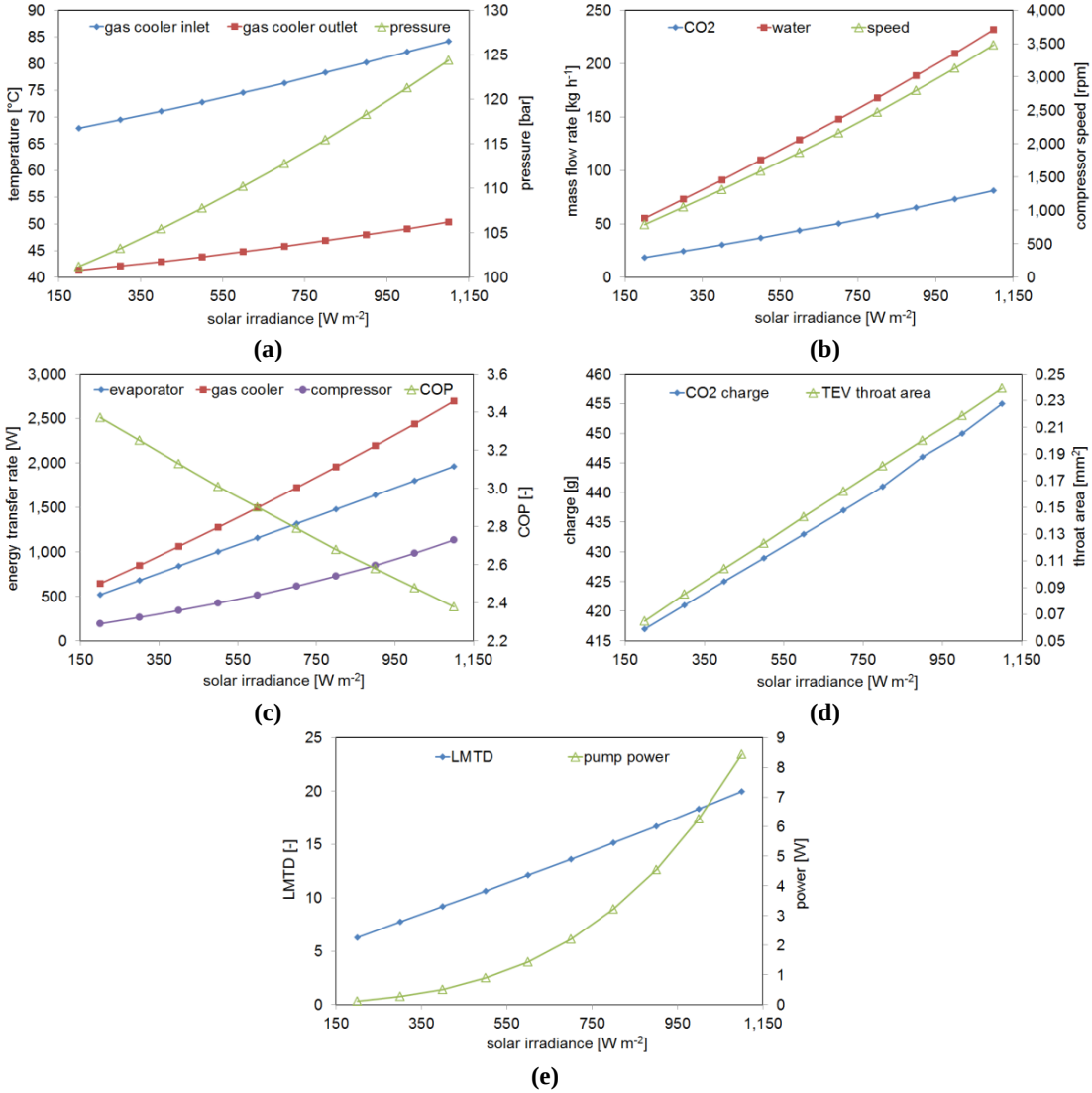

Fig. 5: Results for variation of the solar global irradiance: (a) temperatures and pressure at gas cooler; (b) mass flow rates and compressor speed; (c) heat transfer rates, compressor and pump power and COP; (d) expansion valve aperture and refrigerant charge; (e) LMTD and pump power.

Fig. 6 shows the results for the variation of the water temperature at the gas cooler inlet. As $T_{WATER,in}$ increases pressure and temperature at the gas cooler must also increase, thus greatly affecting the compressor power and severely impairing the COP, although the heat transfer to the water was increased. It is possible to see that although the compressor speed increases steadily because of the raising of the pressure ratio, the TEV needs to adjust to maintain the superheating degree constant.

Figure 6(f) shows profiles for the CO_2 specific heat along the gas cooler as a function of its temperature, for 3 different values of $T_{WATER,in}$. It can be seen that, as the transcritical CO_2 temperature gets closer to the critical point (31°C) there is a strong increase of the specific heat and therefore of the heat capacity of the fluid. Thus, it is recommended to work with the pressure at the high side as close as possible to the critical point in order to achieve higher thermal capacitance and heat transfer efficiency.

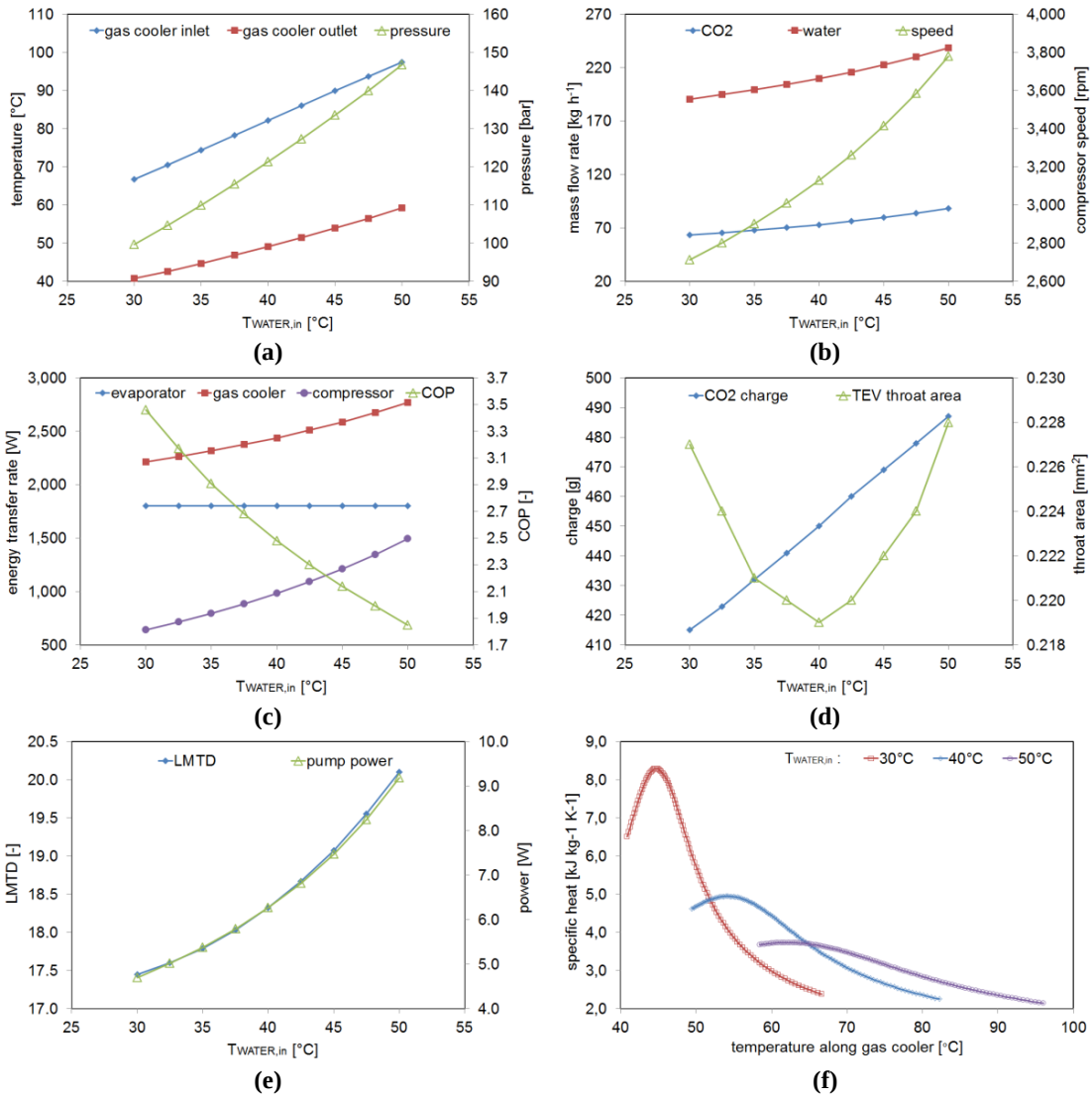

Fig. 6: Results for variation of $T_{WATER,in}$: (a) temperatures and pressure at gas cooler; (b) mass flow rates and compressor speed; (c) heat transfer rates, compressor and pump power and COP; (d) expansion valve aperture and refrigerant charge; (e) LMTD and pump power; (f) profiles for the specific heat of CO_2 along the gas cooler.

As a whole, it is possible to observe that the computational model is robust and presents a consistent response to the variations of the parameters. From the results, it is possible to conclude that, for increasing the COP of the system, it is recommended that:

- evaporating temperature should be maintained equal to the ambient temperature, in order to avoid heat losses to the air, and at the same time maintaining the evaporating pressure as high as possible, what is desirable for reducing compression power;
- the superheating degree at the evaporator outlet should be high, since its effect on the refrigerant density at the compressor suction is small and, since the evaporating pressure must be controlled, higher superheating will allow lower refrigerant mass flow rate;
- $T_{WATER,in}$ should be as low as possible, in order to allow the refrigerant to operate as close as possible to the critical point at the gas cooler, thus improving its heat transfer capacity;

The proposed control strategy showed the ability to achieve an increase in the system COP with reduced

solar irradiance, which is a welcome feature since a real system will operate much of its time under varying solar irradiance conditions.

It must be remembered that this analysis was focused on the efficiency of the heat pump system and not in meeting the hot water demand, that is not being considered here but will be in a future work.

5. Conclusions

In the present work, modeling and a parametric analysis of a solar assisted heat pump for water heating system using CO_2 in a transcritical cycle was carried out. The developed model achieved convergence in a wide operational range and presented results consistent with those in the literature.

The analysis comprised four degrees of freedom or control parameters of the system: (1) restriction on the thermostatic expansion valve (represented by the superheating degree at the evaporator outlet); (2) optimum high pressure (equivalent to setting up the refrigerant charge of the system); (3) water mass flow rate and temperature at the gas cooler inlet (directly related to the demand of hot water); and (4) difference between the evaporation temperature and the ambient temperature in the solar collector (which is adjusted by the control over the compressor speed). The increase in superheat increased the COP, while variations in the temperature difference at the evaporator showed a point of maximum COP when evaporating temperature is close to the ambient temperature.

The influence of the temperature of the water to be heated and solar irradiance were also analyzed, and it was verified a great dependence of the performance of the system on the water inlet temperature in the gas cooler, indicating that this SA-HWHP system may be more adaptable to some types of demand than others. Also, there was a reduction of the COP with the increase of the irradiance although the amount of the heat carried by the heat pump increases.

The behavioral trends of the system showed the feasibility of using CO_2 as working fluid in heat pumps. A better adaptation of the cycle to the peculiar properties of the fluid becomes essential for the system to be more competitive. In addition, a demand-driven analysis and optimization processes is a path that must be followed.

The developed model demonstrated its ability to be used as a design and analysis tool. Notwithstanding, there is room for improvement, such as more detailed and realistic component modeling. The ability to simulate different demand profiles will also be welcome, which may allow the development of different control strategies better adapted to each case.

6. Acknowledgments

Authors would like to acknowledge the support from the Federal Institute of Santa Catarina (IF-SC), Campus São José. Special thanks go to prof. Jesué Graciliano da Silva for his help in preparing this article.

7. References

Abreu, S.L., Rocha, S.P., Gonçalves, J.M., 2011. Thermal performance of a compact solar assisted heat pump. ISES Solar World Congress, Kassel.

Buker, M.S., Riffat, S.B., 2016. Solar assisted heat pump system for low temperature water heating applications: a systematic review. Renew. Sust. Energ. Rev. 55, 399-413.

Calm, J.M., 2008. The next generation of refrigerants – historical review, considerations, and outlook. Int. J. Refrig. 31(7), 1123-1133.

Chen, J.F., Dai, Y.J., Wang, R.Z., 2016. Experimental and theoretical study on a solar assisted CO_2 heat pump for space heating. Renew. Energy 89, 295-304.

De Noni, B., Abreu, S.L., Gonçalves, J.M., 2018. Simulation of a CO_2 heat pump with flat plate solar collector evaporator. VII Brazilian Congress of Solar Energy, Gramado (in portuguese).

EPE - Energy research company, 2012. Technical note DEA 16/12: Energy Efficiency Assessment for the

next 10 years (2012-2021). Ministry of Mines and Energy: Rio de Janeiro (in portuguese).

European Commission, 2007. The Montreal Protocol. Office of Official Publications of the European Communities, Luxembourg.

Hawlader, M.N.A., Chou, S.K., Ullah, M.Z., 2001. The performance of a solar assisted heat pump water heating system. Appl. Therm. Eng. 21, 1049-1065.

Incropera, F.P., De Witt, D.P., 1990. Fundamentals of heat and mass transfer. 2 ed. John Wiley, New York.

Kakaç, S., Liu, H., 2002. Heat exchangers: selection, rating, and thermal design. 2 ed. CRC, Boca Raton.

Klein, S.A., 2002. EES Engineering Equation Solver. Available at: <http://fchart.com/ees/>.

Li, H., Braun, J.E., Shen, B., 2004. Modeling adjustable throat-area expansion valves. International Refrigeration and Air Conditioning Conference, Purdue.

Liao, S.M., Zhao, T.S., Jakobsen, A., 2000. A correlation of optimal heat rejection pressures in transcritical carbon dioxide cycles. Appl. Therm. Eng. 20(9), 831-841.

Lorentzen, G., 1995. The use of natural refrigerants: a complete solution to the CFC/HCFC predicament. Int. J. Refrig. 18(3), 190-197.

Montagner, G.P., Melo, C., 2014. A study on carbon dioxide cycle architectures for light-commercial refrigeration systems. Int. J. Refrig. 42, 90-96.

Nawaz, K., Shen, B., Elatar, A., Baxter, V., Abdelaziz, O., 2018. Performance optimization of CO_2 heat pump water heater. Int. J. Refrig. 85, 213–228.

Passos, L.A., Abreu, S.L., Silva, A.K., 2017. Optimal scale of solar-trough powered plants operating with carbon dioxide. Appl. Therm. Eng. 124, 1203-1212.

Paulino, T.F, Oliveira, R.N., Maia, A.A.T., Palm, B., Machado, L., 2019. Modeling and experimental analysis of the solar radiation in a CO_2 direct expansion solar-assisted heat pump. Appl. Therm. Eng. 148, 160-172.

Peñarrocha, I., Llopis, R., Tárrega, L., Sánchez, D., Cabello, R., 2014. A new approach to optimize the energy efficiency of CO_2 transcritical refrigeration plants. Appl. Therm. Eng. 67, 137-146.

Sun X., Dai, Y., Novakovic, V., Wu, J., Wang, R., 2015. Performance comparison of direct expansion solar-assisted heat pump and conventional air source heat pump for domestic hot water. Energy Procedia 70, 394-401.

Zhang, J., Qin, Y., Wang, C., 2015. Review on CO_2 heat pump water heater for residential use in Japan. Renew. Sust. Energy Rev. 50, 1383-1391.